

The study of polystyrene surface swelling by quartz crystal microbalance and Rutherford backscattering techniques

RADE OGNJANOVIC, C.-Y. HUI*, E. J. KRAMER

*Department of Materials Science and Engineering, and the Materials Science Center, Bard Hall, Ithaca, and *Department of Theoretical and Applied Mechanics, Kimble Hall, Cornell University, Ithaca, New York 14853-1501, USA*

A quartz crystal microbalance technique (QCM) was used to measure the mass gain of a glassy polystyrene film as 1-iodo-*n*-hexane (IOH) was diffused into it. We present a technique by which $\phi_s(t)$, the time dependent volume fraction of IOH at the surface of the PS film, can be obtained from the QCM data. The surface swelling data thus obtained are shown to be in good agreement with values of $\phi_s(t)$ measured independently by Rutherford backscattering spectrometry (RBS). The QCM method has the advantage that the data are obtained continuously from one sample rather than requiring the tedious exposure and analysis of the multiple samples that the RBS method does; it is, however, sensitive to small errors in determining the mass gain rate.

1. Introduction

The diffusion of mid-sized organic molecule "penetrants" into glassy amorphous polymers normally occurs by a non-Fickian diffusion process, called Case II diffusion [1]. In the early stages of sorption, or for all times at very low penetrant activity, the shape of the volume fraction-depth profile is nearly Fickian, i.e.

$$\phi(x, t) = \phi_s \operatorname{erfc} \left[\frac{x}{2(Dt)^{1/2}} \right] \quad (1)$$

where x is the depth below the surface, D is the diffusion coefficient of the penetrant in the polymer glass and ϕ_s is the polymer volume fraction of the penetrant [2]. However, on successive exposures one finds that ϕ_s is not the constant value required if local equilibrium has been attained but slowly increases with time as $\phi_s(t)$. Once a certain critical value of ϕ_s is reached the diffusion coefficient increases by several orders of magnitude to D_R and a sharp front begins to move through the sample at a constant velocity. The swollen polymer behind this Case II front is rubbery and has a constant concentration of penetrant extending from the polymer surface to the boundary between the rubber and glass. In the Thomas and Windle [3] model of Case II diffusion, the slow swelling rate $d\phi_s/dt$ is due to the slow mechanical response of the glassy polymer chains to the osmotic pressure imposed by the difference in penetrant activities just outside and inside the surface. This swelling rate governs not only the time for the Case II front to form, the induction time, but also the steady velocity, V , of the front which is predicted to be [4]

$$V = \left(D \left. \frac{d \ln \phi}{dt} \right|_{\phi_{\text{crit}}} \right)^{1/2} \quad (2)$$

where $d \ln \phi/dt|_{\phi_{\text{crit}}}$ is the value at the maximum in the osmotic pressure ahead of the front. Thus, in order to test and use the TW model one needs to describe the polymer swelling behaviour as a function of time. The simple linear viscous swelling law originally proposed by the TW model has already been shown to be inadequate, but tests of more realistic models of surface swelling are hampered by the difficulty in obtaining accurate data on polymer surface swelling.

In this paper we offer a new method of interpreting data from a quartz crystal microbalance (QCM) to deduce the variation of surface concentration with time at the vapour/polymer interface. The QCM is a very sensitive mass balance which can accurately measure tenths of nanogram mass changes in a polymer as it absorbs solvent vapour. The QCM can therefore be considered as an improvement over the traditional gravimetric experiments [5-8] in which a polymer sample was hung on the end of a quartz fibre spring and the extension of the spring recorded in order to follow the mass change of the sample as it gained weight on exposure to a solvent vapour. That technique had a resolution of the order of micrograms. However, in common with these previous gravimetric techniques, the QCM can only measure the total mass gain of the polymer sample, which alone is not sufficient to determine the surface mass gain as a function of time. In this work, we show that if we use the fact that at low volume fractions the diffusion of 1-iodo-*n*-hexane (IOH) is approximately Fickian [2, 9, 10], then the surface swelling function can be recovered from the measured QCM data. We will compare surface concentration data as found from QCM and Rutherford backscattering spectrometry (RBS) to show that the techniques give equivalent results.

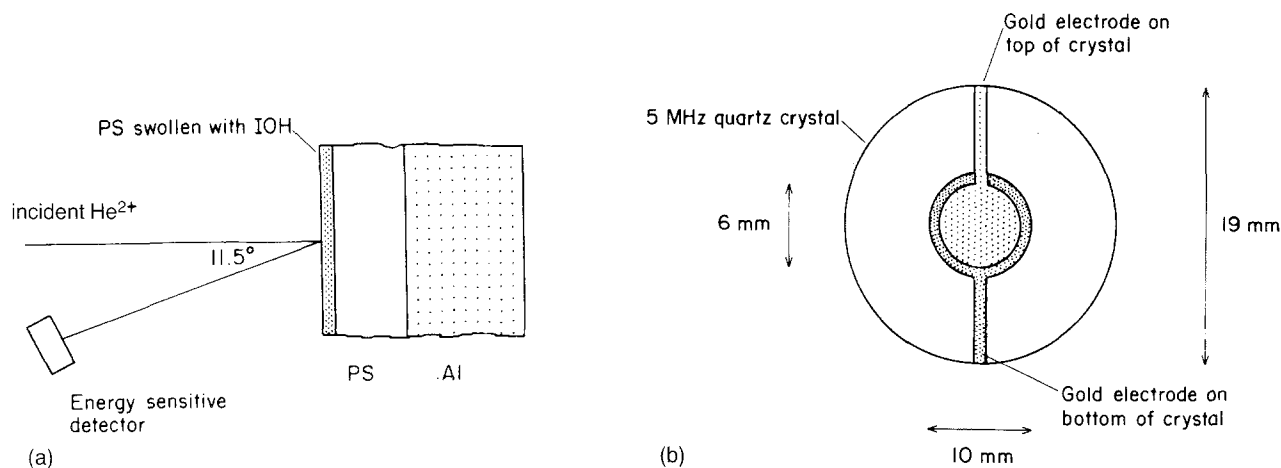


Figure 1 (a) RBS geometry used in our experiment. (b) Schematic drawing of a quartz crystal.

2. Experimental procedure

Films of polystyrene (PS) of various thicknesses were either spun cast on the quartz crystal (for QCM) or cast on an aluminium substrate (for RBS) from a few drops of polymer solution. The PS had a weight average molecular weight of 390 000, a polydispersity index of less than 1.1, and was purchased from Pressure Chemical Company. The PS was dissolved in toluene (ca. 10 wt %) and the film thickness varied by changing the polymer solution concentration.

2.1. RBS Technique

The RBS technique has been described elsewhere [2, 4] but a short description is included here. The experimental arrangement employed here used the geometry shown in Fig. 1a. A 2.4 MeV He^{2+} ion beam impinges on to a smooth sample surface. Some of the backscattered He^{2+} ions are collected by an energy-sensitive detector connected to a multichannel analyser which records the number of ions versus the energy spectrum. The spectrum is then analysed to give information on the elemental composition as a function of depth into the sample from the surface.

Elemental information comes from the energy of the He^{2+} ion scattered from a target nucleus [11]. From the conservation of momentum and energy, the energy of a He^{2+} ion of mass m_i just after it is backscattered through an angle of 180° by a target nucleus of mass M at the sample surface will be

$$E = KE_0 \quad (3)$$

where E_0 is the energy of the incident beam just prior to collision and K the kinematic factor

$$K = [(M - m_i)/(M + m_i)]^2 \quad (4)$$

If the target nucleus is below the surface the He^{2+} ions lose energy in electronic collisions on their way into and out of the sample [12, 13]. Hence the scattering from the target nucleus below the surface appears at lower energy than from one at the surface and this fact can be used to determine the contribution of the target nuclei as a function of depth from the backscattering spectrum using standard algorithms [11, 14–16].

The particular PS/IOH system was chosen to fulfil a number of experimental criteria. Originally this surface swelling study was part of an investigation of

Case II diffusion which PS/IOH can show at high activities of IOH. The polymer is relatively resistant to radiation damage by He^{2+} ions and the iodine atom acts as a convenient tag atom that can be followed by RBS down to a depth of about $4\ \mu\text{m}$ from the PS surface before the iodine signal overlaps the carbon signal. The absence of atoms heavier than carbon in PS allows a good separation of the carbon and iodine energy signals. Iodine also has a large scattering cross-section enabling IOH to be measured to quite low concentrations.

2.2. Polymer samples for RBS

Polymer samples were prepared by casting a polymer film more than $10\ \mu\text{m}$ thick on to Al substrates from solution. These substrates measured $1 \times 15 \times 15\ \text{mm}$ and were polished with fine sandpaper to remove scratches then etched in 50 wt % aqueous sodium hydroxide solution to clean and roughen the aluminium surface for better adhesion of the PS. Samples, which were dried in air for at least 12 h before annealing at 130°C in vacuum for 1 h to remove solvent residues, were then aged at 50°C for 24 h to minimize variations in the extent of physical ageing at room temperature.

PS film samples were exposed to different activities of IOH vapours by holding the polymer sample in a flask containing an IOH/PS solution in equilibrium with its vapour maintained at 30°C . After exposure to IOH vapour, the samples for RBS analysis were cooled in liquid nitrogen and this temperature (77 K) was maintained whilst making RBS measurements in order to freeze in the IOH concentration profile and minimize mass loss due to radiation damage by the ion beam.

2.3. Quartz crystal microbalance

A QCM consists of a quartz crystal vibrating at its resonant frequency and works on the principle that the frequency will decrease when the quartz oscillator surface is coupled to a load. In this experiment the load is a thin film of PS cast on one surface of the crystal which absorbs IOH during an experimental run. The QCM, used for vacuum deposition rate monitors where the coating can be considered to be lossless, is well understood (by lossless we mean there

is little or no attenuation of acoustic waves through the thickness of the coating). Sauerbrey and other authors [17–19] showed that for thin rigid films on the quartz surface the resonant frequency changes linearly with the film mass up to mass loadings equal to 2% of the oscillator mass. The mass/frequency relationship can be written as

$$\Delta f = \frac{-2mf_0}{nA(\mu_q \varrho_q)} \quad (5)$$

where Δf is the change in frequency, f_0 frequency without the film, m the mass change, μ_q the quartz shear modulus, ϱ_q the quartz density, A the area of electrode and n an integer representing the oscillating frequency which may be the fundamental resonant frequency of the crystal ($n = 1$), the third harmonic ($n = 3$), etc.

In our experiments a 5 MHz AT cut quartz crystal oscillating at its fundamental frequency was spin coated with a thin film of PS on one face. A schematic drawing of the crystal and its electrodes is shown in Fig. 1b. The PS-coated quartz crystal is then heat treated in the same way as the RBS samples. When the QCM PS layer was exposed in the same manner as RBS samples to various activities of IOH vapour, the resulting drop in resonant frequency could be related to a mass increase caused by IOH being absorbed by the PS film. In order that the simple rigid film approximation could be used, we carried out all our exposures of the PS film only to low activities of IOH (< 17% IOH volume fraction) to avoid making the PS too rubbery which would cause viscous losses that were difficult to interpret. Equation 3 predicts a 1 Hz change in frequency for every 18 ng mass change per cm² of electrode area. We checked the mass/change in frequency relationship by comparing the original PS film thicknesses determined by optical interference microscopy with those determined using the rigid film approximation from the frequency change of the QCM. The two sets of measurements agreed within the experimental error of the interference microscopy measurement (ca. ± 80 nm).

2.4. Surface swelling functions, $\phi_s(t)$, from QCM data

The QCM gives the total change in mass, m , of PS film as a function of time, t . Let $\bar{\phi}(t)$ be the “average concentration” or volume fraction integrated across a film of thickness L , i.e.

$$\bar{\phi}(t) = \frac{\int_0^L \phi(x, t) dx}{L} \quad (6)$$

where x is the depth into the film. The change in mass is related to $\bar{\phi}(t)$ by

$$m = C\bar{\phi}(t) \quad (7)$$

where

$$C \approx \frac{\varrho_{\text{IOH}} m_{\text{PS}}}{\varrho_{\text{PS}}} \quad (8)$$

and where ϱ_{PS} and ϱ_{IOH} are the densities of PS and IOH and m_{PS} is the mass of the PS film. Equations 5 and 7 relate the change of frequency to the average volume

fraction gain in the polymer glass. Knowledge of $\bar{\phi}(t)$, however is not sufficient to determine the surface volume fraction $\phi_s(t) = \phi(x = 0, t)$. To determine $\phi_s(t)$, we make the assumption that diffusion is Fickian, i.e. $\phi(x, t)$ satisfies the partial differential equation

$$D \frac{\partial^2 \phi}{\partial x^2} = \frac{\partial \phi}{\partial t} \quad 0 < x < L \quad (9)$$

with D as the diffusion coefficient. The appropriate boundary conditions for our experiment are

$$\phi(x = 0, t) = \phi_s(t) \quad (10)$$

$$\frac{\partial \phi(x = L, t)}{\partial x} = 0 \quad (11)$$

with the initial condition

$$\phi(x, t = 0) = 0 \quad 0 < x < L \quad (12)$$

The assumption that $\phi(x, t)$ satisfies the Fickian diffusion equation is justified by previous RBS data which indicate that for equilibrium volume fractions less than ≈ 0.15 , diffusion is approximately Fickian although the surface volume fraction increases with time [2]. We show in Appendix 1 that $\phi_s(t)$ can be determined from Equations 9 to 12 and $\bar{\phi}(t)$. The resulting $\phi_s(t)$ is given by

$$\begin{aligned} \phi_s(t) = & \int_0^t \frac{L}{[\pi(t-t')D]^{1/2}} \\ & \times \left\{ 1 + 2 \sum_{n=1}^{\infty} \exp \left[\frac{-n^2 L^2}{(t-t')D} \right] \right\} \bar{\phi}'(t') dt' \end{aligned} \quad (13)$$

where $\bar{\phi}'(t)$ is the QCM average volume fraction differentiated with respect to time, i.e.

$$\bar{\phi}'(t) = \frac{d\bar{\phi}}{dt} \quad (14)$$

Once $\phi_s(t)$ is found, the diffusion profile $\phi(x, t)$ can be calculated by the following expression,

$$\begin{aligned} \phi(x, t) = & \int_0^t \phi_s(t') \sum_{n=0}^{\infty} \frac{L^3 (-1)^n}{2[\pi(t-t')^3 D^3]^{1/2}} \\ & \times \left\{ (2n+x) \exp \left[\frac{-(2n+x)^2 L^2}{4D(t-t')} \right] \right. \\ & + (2n+2-x) \\ & \left. \times \exp \left[\frac{-(2n+2-x)^2 L^2}{4D(t-t')} \right] \right\} dt' \end{aligned} \quad (15)$$

If D and L are known, Equations 13 and 15 give the surface swelling concentration and diffusion profiles from the QCM data $\bar{\phi}(t)$, so that this technique can be quantitatively compared with RBS.

3. Results and discussion

Typical QCM data shown in Fig. 2 give the total mass change of PS film as a function of time. From previous RBS data for IOH volume fractions less than 10%, D is found to be approximately 1.0×10^{-13} cm² sec⁻¹. In our experiment L is determined by the

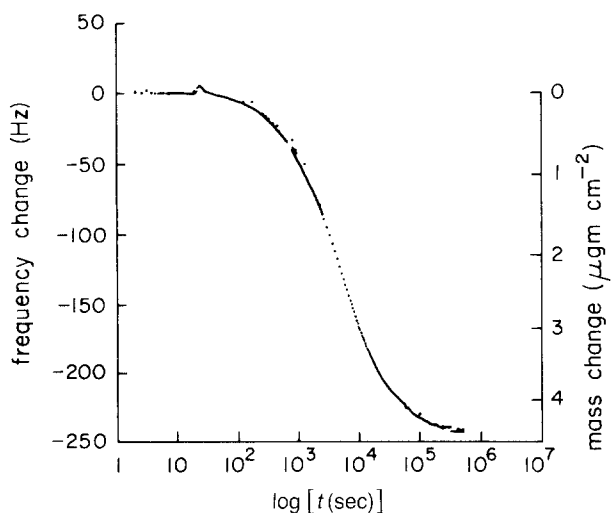


Figure 2 Change in frequency and mass plotted against log (time) for a 423 nm thick PS film exposed to IOH vapour at 30°C. The volume fraction of IOH in equilibrium with the vapour is 0.083.

change in crystal resonant frequency on casting a PS film onto a clean quartz crystal. These values are used to find $\bar{\phi}(t)$ and $\phi_s(t)$ from Equations 6 and 13. These functions, derived from the QCM data in Fig. 2 are shown in Fig. 3. Because $\phi_s(t)$ is very sensitive to relative errors in $\bar{\phi}'(t)$ and these errors become large when $\bar{\phi}'(t)$ becomes small at long times, $\phi_s(t)$ tends to exhibit considerable scatter at long times as shown in Fig. 3.

If Equation 13 is correct, $\phi_s(t)$ should be independent of the PS film thickness used for an exposure to a given equilibrium concentration. In particular, for very thin PS films, $\phi_s(t) \approx \bar{\phi}(t)$ because the film is so thin that a change in IOH concentration at the surface is very quickly transmitted across such a thin section of film. These statements are confirmed by the QCM data in Fig. 4. The $\phi_s(t)$ derived from the QCM data on the thick PS film is consistent with the $\phi_s(t)$ derived from the QCM data on the thinnest PS film.

In order to compare $\phi_s(t)$ from the QCM to those from RBS we calculated concentration profiles from $\phi_s(t)$ using Equation 15 and convoluted these profiles with a Gaussian function equivalent to the RBS instrument depth resolution of 75 nm full-width at

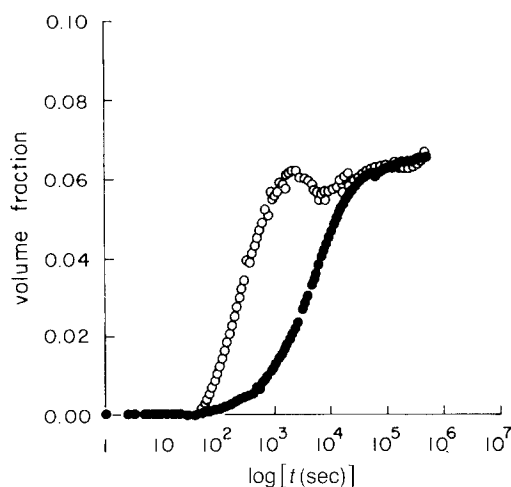


Figure 3 (○) The surface volume fraction of IOH, $\phi_s(t)$, and (●) the average volume fraction of IOH in a PS film plotted against log (time) from the data in Fig. 2.

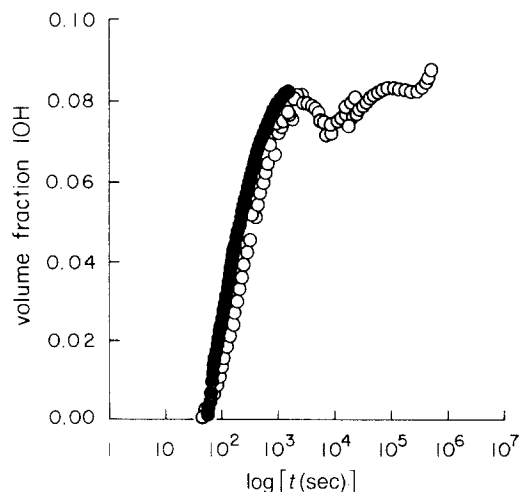


Figure 4 Thin film ((●) 22 nm thick PS) average volume fraction $\bar{\phi}(t)$ and thick film ((○) 423 nm thick) surface volume fraction plotted against log (time).

half-maximum. The resulting concentration profiles obtained by this procedure are superimposed on real RBS concentration depth profiles shown in Fig. 5 for various values of t . The profiles from the different methods are in reasonable agreement. For short exposure times and low diffusion coefficients we find that the RBS instrumental resolution can affect the value of $\phi_s(t)$ measured by this method. We have found that one can improve the accuracy here by optimising RBS instrument parameters for higher depth resolution by tilting the sample normal so it makes large angles to the incident beam [11] so that the He^{2+} ions have to travel through more polymer to reach a certain depth normal to the PS surface. For diffusion at long times the effect of RBS resolution on the apparent surface IOH concentration is small.

We have also investigated the possible desorption of the surface IOH in the RBS sample during the process of transferring the sample from the flask into liquid nitrogen. The transfer process takes a maximum of 2 sec. To investigate the effect of desorption, RBS spectra were measured where the sample was removed

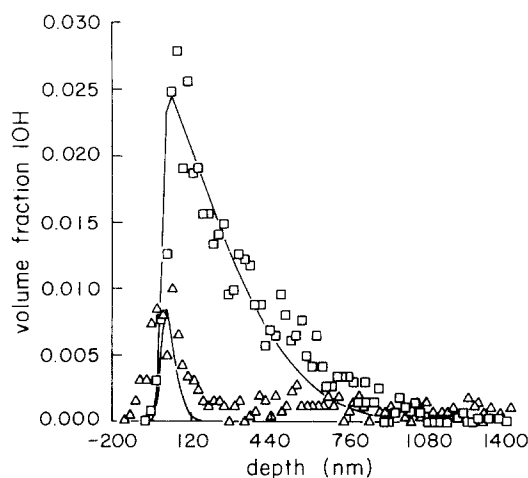


Figure 5 Iodohehexane volume fraction plotted against depth profiles measured by RBS after the PS film was exposed to IOH vapour for (Δ) 326 sec and (□) 7201 sec. The equilibrium volume fraction was ≈ 0.08 . The solid lines are calculated profiles derived from the QCM swelling data using Equations 11 and 13.

from the flask and held in air for 2, 6 and 12 sec before freezing. Very little difference in surface concentrations was found due to desorption of the IOH.

4. Conclusions

We have shown that QCM measurements, coupled with the use of Equation 13, give surface concentrations in good agreement with those obtained from RBS. QCM has some distinct advantages over RBS: the QCM method has a very high sensitivity and can collect swelling data continuously in time. The QCM method for determining $\phi_s(t)$ has the disadvantage that it is sensitive to the derivative of the experimental $\bar{\phi}(t)$ data so that the derived $\phi_s(t)$ becomes quite noisy at long times. The RBS method can be used to obtain concentration–depth profiles directly and thus was used here to measure the Fickian diffusion coefficient of PS needed for the QCM calculations.

Acknowledgements

We thank Owen Melroy, IBM Almaden Research Laboratory, for introducing us to the QCM technique, coating the quartz crystals with gold electrodes and guidance in developing a working system. We thank Tom Gall for helpful discussions on the QCM technique. The support of the US Army Research Office, Durham (R.O. and E.J.K.) and the Cornell Materials Science Centre (C.Y.H.) which is funded by the NSF–DMR–MRL programme is gratefully acknowledged.

Appendix

The problem is to deduce $\phi_s(t)$ given $\bar{\phi}(t)$ for $t > 0$. Laplace transformation of Equation 9 using the initial condition, Equation 12, gives

$$D \frac{\partial^2 \bar{\phi}}{\partial x^2} + s\bar{\phi} = 0 \quad (\text{A1})$$

where \sim denotes the Laplace transform of $\phi(x, t)$ with respect to the transform variable s . The two arbitrary constants in the solution of Equation A1 are determined uniquely by the Laplace transform of the boundary conditions given by Equations 10 and 11, resulting in

$$\bar{\phi}(x, s) = \bar{\phi}_s(s) \left[\frac{\cosh\left(\frac{s}{D}\right)^{1/2} (L-x)}{\cosh\left(\frac{s}{D}\right)^{1/2} L} \right] \quad (\text{A2})$$

Integrating both sides of Equation A2 from $x = 0$ to L and dividing the resulting expression by L we find

$$\bar{\phi}(s) = \frac{D^{1/2} \bar{\phi}_s(s)}{L s^{1/2}} \tanh\left(\frac{s}{D}\right)^{1/2} L \quad (\text{A3})$$

Solving for $\bar{\phi}_s(s)$ in Equation A3, we have

$$\bar{\phi}_s(s) = \frac{L}{(sD)^{1/2}} s\bar{\phi}(s) \coth\left(\frac{s}{D}\right)^{1/2} L \quad (\text{A4})$$

Application of the convolution theorem to Equation A4 gives

$$\phi_s(t) = \int_0^t H(t-t') \bar{\phi}'(t') dt' \quad (\text{A5})$$

where $H(t)$ is the inverse Laplace transform of

$$\left(\frac{1}{sD}\right)^{1/2} L \coth\left(\frac{s}{D}\right)^{1/2} L = \frac{L}{(sD)^{1/2}} \times \left\{ 1 + 2 \sum_{n=1}^{\infty} \exp\left[-2n\left(\frac{s}{D}\right)^{1/2} L\right] \right\}$$

which is

$$\frac{L}{(\pi Dt)^{1/2}} \left[1 + \sum_{n=1}^{\infty} \exp\left(\frac{-n^2 L^2}{Dt}\right) \right] \quad (\text{A6})$$

An equivalent expression for $H(t)$ which is particularly useful for long times is

$$\left[1 + 2 \sum_{n=1}^{\infty} \exp\left(\frac{-Dn^2 \pi^2 t}{L^2}\right) \right] \quad (\text{A7})$$

If $\phi_s(t)$ is known, the solution of Equations 7 to 10 is obtained by direct inversion of Equation A2, which is

$$\phi(x, t) = \int_0^t \phi_s(t') \sum_{n=0}^{\infty} \frac{L^3 (-1)^n}{2[\pi(t-t')^3 D^3]^{1/2}} \left\{ (2n+x) \exp\left[\frac{-(2n+x)^2 L^2}{4D(t-t')}\right] + (2n+2-x) \times \exp\left[\frac{-2n+2-x)^2 L^2}{4D(t-t')}\right] \right\} dt'$$

References

1. T. ALFREY, E. F. GURNEY and W. G. LLOYD, *J. Polym. Sci. Polym. Symp.* **C12** (1966) 249.
2. R. C. LASKY, E. J. KRAMER and C.-Y. HUI, *Polymer* **29** (1988) 673.
3. N. L. THOMAS and A. H. WINDLE, *ibid.* **23** (1982) 529.
4. P. J. MILLS, C. J. PALMSTROM and E. J. KRAMER, *J. Mater. Sci.* **21** (1986) 1479.
5. S. PRAGER and F. A. LONG, *J. Amer. Chem. Soc.* **73** (1951) 4072.
6. C. H. M. JACQUES and H. B. HOPFENBERG, *Polym. Engng. Sci.* **14** (1974) 441.
7. D. J. ENSCORE, H. B. HOPFENBERG and V. T. STANNETT, *Polymer* **18** (1977) 793.
8. A. R. BEVENS and H. B. HOPFENBERG, *ibid.* **19** (1978) 489.
9. C. Y. HUI, K. C. WU, R. C. LASKY and E. J. KRAMER, *J. Appl. Phys.* **61** (1987) 5129.
10. *Idem, ibid.* **61** (1987) 5137.
11. W. K. CHU, J. W. MAYER and M. A. NICOLET, "Backscattering Spectrometry" (Academic, New York, 1987) Chs 2, 3.
12. J. F. ZIEGLER, "The Stopping and Ranges of Ions in Matter", Vol. 4 (Pergamon, New York, 1977).
13. H. ANDERSON and J. F. ZIEGLER, "The Stopping and Ranges of Ions in Matter", Vol. 3 (Pergamon, New York, 1977).
14. L. R. DOOLITTLE, *Nucl. Instrum. Meth.* **B9** (1985) 344.
15. *Idem, ibid.* **B15** (1986) 227.
16. J. F. ROMANELLI, J. W. MAYER and E. J. KRAMER, *J. Polym. Sci. Polym. Phys. Edn.* **24** (1986) 263.
17. G. SAUERBREY, *Z. Physik* **155** (1959) 206.
18. K. H. BEHRNDT, *J. Vac. Sci. Technol.* **8** (1971) 622.
19. C. D. STOCKBRIDGE, in "Vacuum Microbalance Techniques", Vol. 5, edited by K. Behrndt (Plenum Press, New York, 1966) 193.

Received 28 September 1988
and accepted 28 February 1989